Drug Design, Development and Therapy

Dovepress
Taylor & Francis Group

Open Access Full Text Article

ORIGINAL RESEARCH

Anti-Inflammatory Modified Fuzi Decoction Antagonizes Synovial TNF-α/TRAF2/NF-κB Signaling to Remedy Osteoarthritis

Yue Wang[1,2,*], Jiadan Ren[1,*], Huixin Chen[1], Xiaotian Chen[1], Bo Yan[1], Wenting Xu[2], Xiujuan Xiao[1], Qiang Yuan[1], Letian Shan[2,3], Li Zhou[2]

[1]College of Pharmaceutical Sciences, Zhejiang Chinese Medical University, Hangzhou, 310053, People's Republic of China; [2]The First Affiliated Hospital of Zhejiang Chinese Medical University (Zhejiang Provincial Hospital of Chinese Medicine), Hangzhou, 310053, People's Republic of China; [3]Fuyang Research Institute, Zhejiang Chinese Medical University, Hangzhou, 310053, People's Republic of China

*These authors contributed equally to this work

Correspondence: Qiang Yuan; Li Zhou, Email yuanqiang0825@sina.com; zhouli@zcmu.edu.cn

Purpose: To assess the pharmacodynamic effects and therapeutic mechanisms of modified Fuzi decoction (MFZD) in osteoarthritis (OA), particularly OA-related inflammation.

Methods: The main components of MFZD were identified using Ultra Performance Liquid Chromatography-Tandem Mass Spectrometry (UPLC-MS/MS). An OA model was established in Sprague-Dawley rats via intra-articular injection of monoiodoacetate (MIA) to evaluate the anti-OA efficacy of MFZD via gavage. In vivo studies, including pain behavior evaluation, histopathological observation, immunohistochemical analysis, enzyme-linked immunosorbent assay (ELISA), Meso Scale Discovery (MSD), and Western blot (WB), were carried out to demonstrate the anti-inflammatory and anti-degenerative potency of MFZD against OA. Potential targets and pathways of MFZD were identified via network pharmacology analysis and Kyoto Encyclopedia of Genes and Genomes (KEGG) pathway enrichment, respectively. Subsequently, the tumor necrosis factor (TNF) signaling and related targets were validated in vitro by WB. For in vitro validations, primary synovial fibroblasts were isolated from rats and treated with MFZD-containing serum (MFCS) in the presence of TNF-α.

Results: UPLC-MS/MS analysis identified key compounds in MFZD, including trans-cinnamaldehyde, atractylenolide I, lobetyolin, paeoniflorin, pachymic acid, carmichaeline, talatisamine, fuziline, benzoylhypacoinine, benzoylmesaconine, benzoylaconine, hypaconitine, deoxyaconitine, mesaconitine, and aconitine. MFZD treatment improved the paw withdrawal threshold (PWT), alleviated histopathological damage, reduced TNF-α and monocyte chemotactic protein-1 (MCP-1) in the serum, and remedied the abnormal anabolism/catabolism of cartilage. TNF signaling was identified through network pharmacology analysis as the anti-inflammatory mechanism of MFZD, and validated by WB results showing that MFCS treatment reduced TNF-α-induced protein expression of p-MKK3/MKK6, p-p38, TRAF2, p-p65, and VCAM1.

Conclusion: This study demonstrated that MFZD exerts anti-degenerative and anti-inflammatory potency against OA and revealed the TNF-α/TRAF2/NF-κB signaling related anti-inflammatory mechanism of MFZD for the first time, offering mechanistic insights into its potential in OA therapy.

Keywords: modified Fuzi decoction, osteoarthritis, synovitis, network pharmacology, TNF-α/TRAF2/NF-κB signaling

Introduction

Osteoarthritis (OA) is a disabling disease affecting the elderly, characterized by degeneration of the whole joint,[1] and is recognized as one of the leading causes of disability in adults. Over 500 million people worldwide are estimated to be affected by OA.[2,3] The increasing incidence and prevalence of OA will certainly cause heavy health and financial burdens on society.[4,5] At present, in addition to lifestyle changes, the clinical treatment for early OA is mainly based on oral or topical non-steroidal anti-inflammatory drugs, corticosteroid injections, and other symptomatic relief programs, which cannot effectively delay the

Received: 18 February 2025
Accepted: 23 August 2025
Published: 2 September 2025

Graphical Abstract

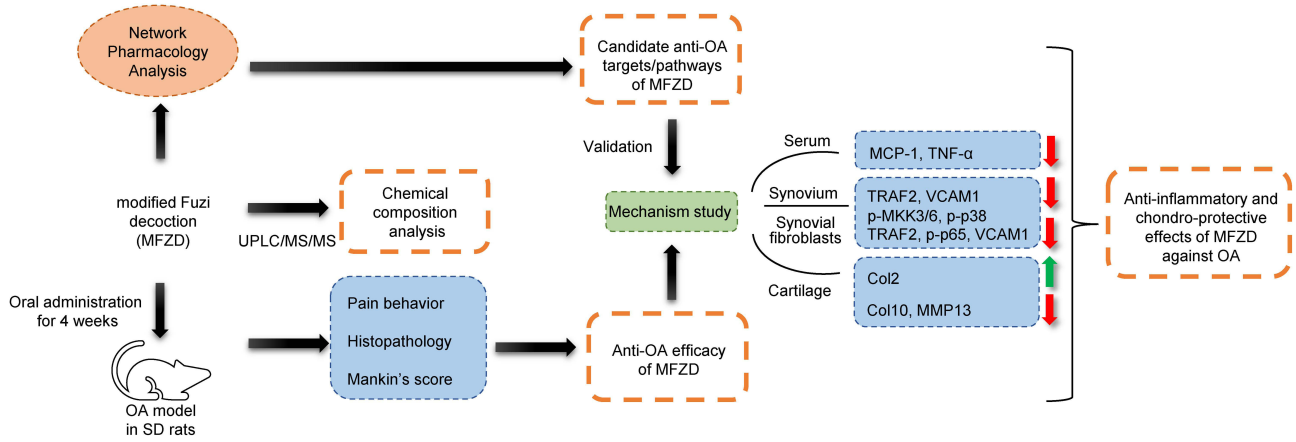

progression of OA and have certain side effects.[6] When OA progresses to the advanced stage, only surgical treatment such as joint replacement can be used, which is expensive and has poor therapeutic effect.[7–9] Therefore, there is an urgent need to develop treatments that alleviate symptoms and delay the progression of OA.

Limited joint activity and pain are the main symptoms of OA, which are closely related to the destruction of articular cartilage and chronic synovitis.[10–12] Synovitis is not confined to the late stages of OA and may even be associated with cartilage damage during the early stages.[13] Synovitis can lead to the release of catabolism and pro-inflammatory mediators, such as cytokines and nitric oxide, and break the catabolism/anabolic balance of the cartilage matrix, resulting in excessive cartilage decomposition. In turn, cartilage degradation can further augment synovitis. Therefore, synovium-targeted therapy should alleviate disease symptoms and prevent structural progression.[14]

Traditional Chinese medicine (TCM), known as economical and multitargeted therapies with less side-effects, has shown great potential in the treatment of OA.[15] Key bioactive constituents of TCM (including alkaloids, polysaccharides and flavonoids) demonstrate chondroprotective effects by modulating critical pathways such as PINK1/Parkin-mediated mitochondrial autophagy and TLR2/NF-κB signaling pathway.[16–19] Furthermore, TCM formulation Xibining improves synovitis and pain symptoms of OA, as evidenced by decreased macrophage infiltration as well as reduced levels of TRPA1, TRPV1, and TRPM8 levels in animal model.[20] Fuzi decoction (FZD) is a classic TCM prescription first recorded in the typhoid theory and is traditionally used to cure severe and migratory arthralgia (ie, a painful sickness) including OA. Recently, preclinical studies in animal models and clinical trials have been conducted on FZD and have provided evidence for its anti-OA efficacy in improving cartilage degeneration. Both the original and modified FZD (MFZD) have been used to eliminate wind and unblock the yang, warm meridians, and dispel cold, strengthen the spleen, and transform dampness in TCM theory, corresponding to the anti-inflammatory and analgesic pharmacological effects in modern medicine.[21] However, the anti-inflammatory effects and mechanisms of FZD (including MFZD) against OA have not been elucidated to date.[22–24]

Guizhi and Shaoyao, with reported anti-inflammatory and analgesic effects, are frequently added to the original prescription to form MFZD.[25,26] Herbal and active ingredients of MFZD possess anti-inflammatory (eg, Fuzi, Guizhi, Shaoyao, Fuling, and Dangshen),[27–30] antalgic (eg, Fuzi and Fuling),[31] and immunoregulatory (eg, Fuzi and Shaoyao) effects,[32,33] benefiting OA therapy. Previous studies have demonstrated that multiple bioactive ingredients in MFZD (eg, cinnamaldehyde, atractylenolide, lobetyolin, and benzoylaconitine) are capable of suppressing TNF-α production or NF-κB-related pathways, where NF-κB serves as a key transcriptional factor modulating inflammatory responses.[34–38,] However, the comprehensive anti-inflammatory mechanisms of MFZD remain to be elucidated. Therefore, this study aimed to evaluate the anti-inflammatory efficacy and reveal the underlying mechanisms of MFZD in OA therapy. Via network pharmacological analysis as well as experimental validations, our results confirmed the anti-OA efficacy of MFZD and revealed a TNF-α/TRAF2/NF-

κB related anti-inflammatory mechanism. These results imply that MFZD is a potential alternative medicine for OA therapy, with considerable anti-degeneration and anti-inflammatory effects.

Materials and Methods

Reagents

Monoiodoacetate (MIA) was purchased from Sigma-Aldrich (MO, USA). Fuzi was obtained from Sichuan Jiangyou Zhongba Fuzi Technology Development Co., Ltd. (Jiangyou, China), and other Chinese herbs were purchased from Zhejiang Chinese Medical University Chinese Herbal Pieces Co. Ltd (Hangzhou, China). Standard components for each herb were selected according to the Chinese Pharmacopoeia and obtained from Chengdu Must Bio-Technology Co., Ltd. (Chengdu, China). Detailed information regarding the antibodies used is presented in Table 1.

Preparation of MFZD

MFZD consists of seven herbs: 15 g Fuzi, 9 g Fuling, 6 g Dangshen, 12 g Baizhu, 15 g Baishao, 15 g Chishao, 12 g Guizhi. Fuzi was soaked in pure potable water (10 times the weight of Fuzi) for 30 min, boiled, and kept slightly boiling for 1.5 h. Other herbs of the decoction were soaked in pure potable water (10 times the weight of herbs except for Fuzi) for 30 min and mixed with the decoction of Fuzi. The mixture was then boiled until boiling, and kept slightly boiling for 30 min to get the complete decoction. The decoction was filtered with medical gauze and aliquoted into sterilized glass bottles. The herbs boiled in the bottle were added to eight times the weight of pure potable water and boiled again. Finally, the filtrate was mixed, concentrated to 1 g/mL, and stored at 4°C until further use. Specific information of the traditional Chinese medicine is presented in Table 2.

Chemoprofile of MFZD

In this study, we made some modifications to the previously reported protocol, and then developed and validated the conditions for UPLC/MS/MS. An ACQUITY Xevo TQ-XS UPLC-MS system (Waters, Milford, MA, USA) and BEH C18 column (2.1 mm × 100 mm, 1.7 μm) were used for chromatographic separation. The standard components and MFZD samples were diluted for subsequent use. Gradient elution was performed using 5 mM aqueous ammonium formate (mobile phase A) and acetonitrile (mobile phase B) as follows: 0–0.5 min, 10% B; 0.5–1.5 min, 10–30% B;

Table 1 Detailed Information for Antibodies

Target	Source	Cat. No.	Dilution	Application
VCAM1	Abcam	ab134047	1:1000	WB
			1:500	IHC
TRAF2	Proteintech	26846-1-AP	1:1000	WB
			1:400	IHC
MMP13	Novus Biologicals	NBP2 −45887	1:4000	WB
	Abcam	ab219620	1:500	IHC
Col2	Abcam	ab34712	1:200	IHC
Col10	Abcam	ab182563	1:2000	WB
p65	CST	8242	1:1000	WB
p-p65	CST	3033	1:1000	WB
β-actin	Sigam	A3854	1:40000	WB
MKK3/MKK6	ABclonal	A19830	1:1000	WB
p-MKK3/MKK6	ABclonal	AP1449	1:1000	WB
p38	CST	8690	1:1000	WB
p-p38	CST	4511	1:1000	WB
β-Tubulin	CST	5346	1:1000	WB

Abbreviations: Cat. No., catalog number; WB, Western blot; IHC, immunohistochemistry; CST, Cell Signaling Technology.

https://doi.org/10.2147/DDDT.S481770

Table 2 Formula of MFZD

Latin Names	Han Name	English Name	Medical Part	Weight (g)
Aconitum carmichaelii Debx.	Fuzi	Aconiti Lateralis Radix Praeparata	Root	15
Poria cocos (Schw.) Wolf.	Fuling	Poria	Sclerotium	9
Codonopsis pilosula (Franch.) Nannf.	Dangshen	Codonopsis Radix	Root	6
Atractylodes macrocephala Koidz.	Baizhu	Macrocephalae Rhizoma	Rhizome	12
Paeonia lactiflora Pall.	Baishao	Paeoniae Radix Alba	Root	15
Paeonia lactiflora Pall.	Chishao	Paeoniae Radix Rubra	Root	15
Cinnamomum cassia Presl.	Guizhi	Cmnamomi Mmulus	Twig	12

1.5–6 min, 30–70% B; 6–7 min, 70–90% B; 7–8.5 min, 90% B; flow rate, 0.2 mL/min. The injection volume was 5 μL, and the column temperature was 40°C.

In this study, Waters Xevo TQ-XS (Milford, MA, USA) with an ESI source and multiple reaction monitoring (MRM) mode (100–700 m/z) was used for mass spectrometry analysis. Full-scan mass spectrometry results were collected in the positive mode. The following were the optimized mass spectrometry conditions: capillary voltage: 3 kV in (+) mode; cone hole voltage: 30 V; cone hole blowback gas flow rate: 150 L/h; desolvation gas temperature: 500°C; desolvation gas flow rate: 800 L/h.

Animals and Modeling

Specific pathogen-free (SPF) Sprague Dawley (SD) rats were provided by Shanghai Super B&K Laboratory Animal Co. Ltd. (Certificate number: SCXK (Shanghai) 2018–0006). All rats were housed in a standard environment with a 12 h light/dark cycle with free access to food and water. An OA model was established using MIA in rats. Briefly, 50 μL of 15 mg/mL MIA was injected into the joint cavity of both legs of rats. The animal study protocol was approved by the Laboratory Animal Management and Ethics Committee of Zhejiang Chinese Medical University (approval number: 20220815–07) following the Chinese standards for the use and care of experimental animals.

About 28 male SD rats (weighing 200 ± 20 g) were randomly divided into four groups (n = 7 each): Sham, model, MFZD-L, and MFZD-H. Except for the sham group, the other groups of rats received OA modeling via intra-articular injection of 50 μL MIA (15 mg/mL), as previously described, while rats in the sham group were treated with an equivalent volume of saline. One week after OA modeling, rats in MFZD-L and MFZD-H group were treated with low (4.4 g/kg/day) and high dose (8.8 g/kg/day) MFZD by gavage, respectively. The rats in the sham and model groups were administered an equivalent volume of saline. All treatments were performed once daily for four weeks. The dosage was determined by using a conversion formula for crude human and biological drugs. The high dosage was the clinical dosage of MFZD (according to the dosage of Fuzi decoction), and the low dosage was half the clinical dosage of MFZD. After 4 weeks of treatment, blood was collected from each group of rats after anesthesia, and serum was separated for subsequent use.

Sample size estimation was performed using the Resource Equation Method (Festing & Altman, 2002). Based on the target degrees of freedom (DF) range of 10–20 for ANOVA error terms, the total sample size was derived (minimum: 16; maximum: 24). To account for potential attrition such as surgical mortality, 28 rats (7 per group) were used.

Preparation of MFZD-Containing Serum

MFZD-containing serum (MFCS) and blank serum (BS) were obtained from 30 rats. Rats were randomly divided into control and MFZD groups, which were administered pure water or MFZD (8.8 g/kg/day) via oral gavage for 7 days. Blood was collected from the heart 2 h after the last administration and centrifuged at 3000 rpm for 10 min at room temperature to obtain the MFCS and BS. The obtained serum was inactivated at 56°C for 30 min, filtered through a 0.22 μm filter membrane to remove bacteria and stored at −80°C.

Isolation and Culture of the Primary Synovial Fibroblasts (SFs)

SFs were isolated from the synovial tissue of 3-week-old male SD rats (n = 5, weighing 200 ± 20 g). The synovial tissue of the rats was cut, digested with collagenase VIII (10 mg/mL) for 2 h, and then terminated with PBS. The mixture was filtered, centrifuged at 3000 rpm for 10 min at room temperature, resuspended, and cultured in Dulbecco's modified Eagle medium (DMEM) containing 10% FBS.

Cellular Experimentation

The four SF groups were negative control (NC), TNF-α (Model), TNF-α + 5% MFCS (MFZD-L), and TNF-α + 10% MFCS (MFZD-H) groups. The Model, MFZD-L, and MFZD-H groups were pretreated with TNF-α (10 ng/mL) for 24 h. After that, MFZD-L and MFZD-H groups were administered the indicated 5% (supplemented with 5% BS) or 10% MFCS for 24 h, and the NC group was administered BS for 24 h.

Pain Behavior Evaluation

The mechanical allodynia was assessed by von Frey hairs (0.6–60 g, UGO Basile, Italy) using the "Up-Down" test paradigm. Briefly, rats were placed on a metal mesh and separated using an elevated plastic cage. After adapting to the environment, von Frey hairs were pressed vertically and forcefully onto the plantar surface of the two hind paws of each rat to bend them, and the paw withdrawal threshold (PWT) was calculated.[39]

Histopathological and Immunohistochemical Analyses

After the rats were sacrificed, the synovium and joint tissues were removed and fixed with paraformaldehyde solution (4%) for 24 h. The joint tissues were then placed in EDTA solution (10%) for decalcification for 2 months. After decalcification, each sample was embedded in paraffin, cut into 2–3 μm, stained with HE (hematoxylin and eosin), SO (Safranin O/Fast green) and MASSON. Synovitis and cartilage damage severity of OA patients were evaluated using the Krenn and Mankin scoring systems, respectively. The expression of collagen type II (Col2) and matrix metallopeptidase 13 (MMP13) was detected by immunohistochemistry. Briefly, for antigen retrieval, each section was immersed in 0.01 mol/L citrate buffer (pH 6.0, Solarbio, Beijing, China) for 4 h at 60°C and then incubated with different primary antibodies at 4°C overnight. After washing with PBS, each section was incubated with the corresponding secondary antibody at room temperature for 20 min and finally developed with 3,3′-diaminobenzidine (DAB). Quantitative analysis of immunohistochemical staining was performed using distinct methods according to biomarker expression patterns: MMP13 staining was semi-quantitatively scored via the quick score (Q-score) method integrating staining intensity and percentage of positive cells, while Col2 staining was quantified by measuring average optical density (AOD).

Cytokine Assays

Global levels of MCP-1 and TNF-α in the serum were determined by Enzyme-linked immunosorbent assay (ELISA) and Meso Scale Discovery (MSD) assay, respectively.

ELISA kit for monocyte chemotactic protein 1(MCP-1) was purchased from Multi Sciences (Lianke) Biotech Co., Ltd. (Hangzhou, China). Rat serum was collected and diluted to determine the level of MCP-1 according to the manufacturer's instructions.

The whole process of MSD was performed by Shanghai LabEx Biotech Co., LTD. with a commercial kit from Meso Scale Discovery (K15059D-X, MD, USA). Briefly, samples were prepared from rat serum at the dilution ratio of 1:2. Each sample (50 μL) was added to the well of a pre-processed MSD assay plate and incubated at room temperature for 1 h with shaking. Then, 25 μL primary antibody was added and incubated at room temperature for another 1 h with shaking. After washing three times, 150 μL read buffer was added to each well. Finally, the plate was analyzed on MESO QuickPlex (SQ120, Meso Scale Discovery, MD, USA).

Network Pharmacology Analysis

The potential targets and mechanisms of MFZD in OA treatment were explored using network pharmacology. First, the main components and protein targets of the seven Chinese herbs in MFZD were obtained from the TCM Systems Pharmacology Database and Analysis Platform (TCMSP).[40] After screening, the protein names were transformed into gene symbols (Homo sapiens) using the UniProt database (https://www.uniprot.org/).[41] With "osteoarthritis" as the keyword, OA-related targets were searched from databases including Online Mendelian Inheritance in Man (OMIM, https://omim.org/), Drug Bank (https://go.drugbank.com/), GeneCards (https://www.genecards.org/), Disgenet (https://www.disgenet.org) and therapeutic target database (TTD, https://db.idrblab.net/ttd/).[42–45] Cytoscape (v3.7.1, https://www.cytoscape.org/) was used to construct the MFZD-OA-target network. In this network diagram, the chemical components and targets of MFZD are represented by nodes. The "degree" of the node was calculated by the number of connected edges. The functions of the targets were analyzed using the David database (https://david.ncifcrf.gov/). A protein-protein interaction (PPI) network diagram was constructed to screen the core genes of MFZD for OA targeting. The effective components of MFZD were intersected with disease-related target genes, and biological information enrichment analysis, including the Gene Ontology (GO) function and Kyoto Encyclopedia of Genes and Genomes (KEGG) pathway enrichment analysis, were performed using the David online database (https://david.ncifcrf.gov/tools.jsp). GO functions were divided into cellular component (CC), molecular function (MF), and biological process (BP).

Western Blot (WB) Analysis

Cell pellets or ground tissues were lysed on ice with lysis buffer (pH 7.4, 50 mM Tris-HCl, 150 mM NaCl, 1 mM EDTA, 1% Triton, and 0.1% SDS) supplemented with phosphatase and protease inhibitors to extract total proteins. Protein concentrations were determined using a bicinchoninic acid (BCA) kit (Thermo Fisher, USA). The protein samples were denatured and separated by denaturing sodium dodecyl sulfate-polyacrylamide gel electrophoresis (SDS-PAGE, 8~12%) and then transferred onto a nitrocellulose membrane (Sartorius Stedim, Göttingen, Germany). The membranes were incubated with 4% non-fat milk in Tris-buffered saline Tween (TBST) at 4°C for 2 h and then incubated with the indicated primary antibodies at 4°C overnight. The membranes were then washed with TBST and incubated with the corresponding secondary antibodies at 4°C for 2 h. Protein bands were developed using Western Lightning® Plus ECL (Perkin Elmer, Inc., Waltham, MA, USA) and detected using a ChemiDoc XRS+ System (Bio-Rad Laboratories, Inc., USA).

Statistical Analysis

All statistical analyses were performed using GraphPad Prism 9.0 (San Diego, CA). Data are expressed as mean ± standard deviation. Normality (Shapiro–Wilk test) and homogeneity of variance (Brown-Forsythe test) were first assessed. For datasets satisfying both assumptions, one-way ANOVA with Tukey's post hoc test was performed for multi-group comparisons, and Student's *t*-tests were used for comparisons between two groups. Kruskal–Wallis *H*-test or Mann–Whitney *U*-test was utilized where assumptions were violated. Statistical significance was defined as $p < 0.05$.

Results

Chemoprofile of MFZD

First, the chemoprofile and quality of MFZD were determined using UPLC-MS/MS. Here, 15 standards (Figure 1A) for herbs in MFZD were analyzed as references (Figure 1B). All 15 standards were detected in MFZD, and their concentrations were as follows: trans-cinnamaldehyde, 8.239 ± 1.583 μg/mL; atractylenolide I, 0.323 ± 0.088 μg/mL; lobetyolin, 5.556 ± 0.057 μg/mL; paeoniflorin, 3274.646 ± 113.434 μg/mL; pachymic acid, 0.079 ± 0.000 μg/mL; carmichaeline, 1.438 ± 0.121 μg/mL; talatisamine, 0.356 ± 0.042 μg/mL; fuziline, 2.273 ± 0.077 μg/mL; benzoylhypacoinine, 6.773 ± 0.174 μg/mL; benzoylmesaconine, 93.713 ± 7.267 μg/mL; benzoylaconine, 5.070 ± 0.126 μg/mL; hypaconitine, 0.199 ± 0.095 μg/mL; deoxyaconitine, 0.033 ± 0.005 μg/mL; mesaconitine: 0.004 ± 0.001 μg/mL; aconitine: 0.003 ± 0.001 μg/mL.

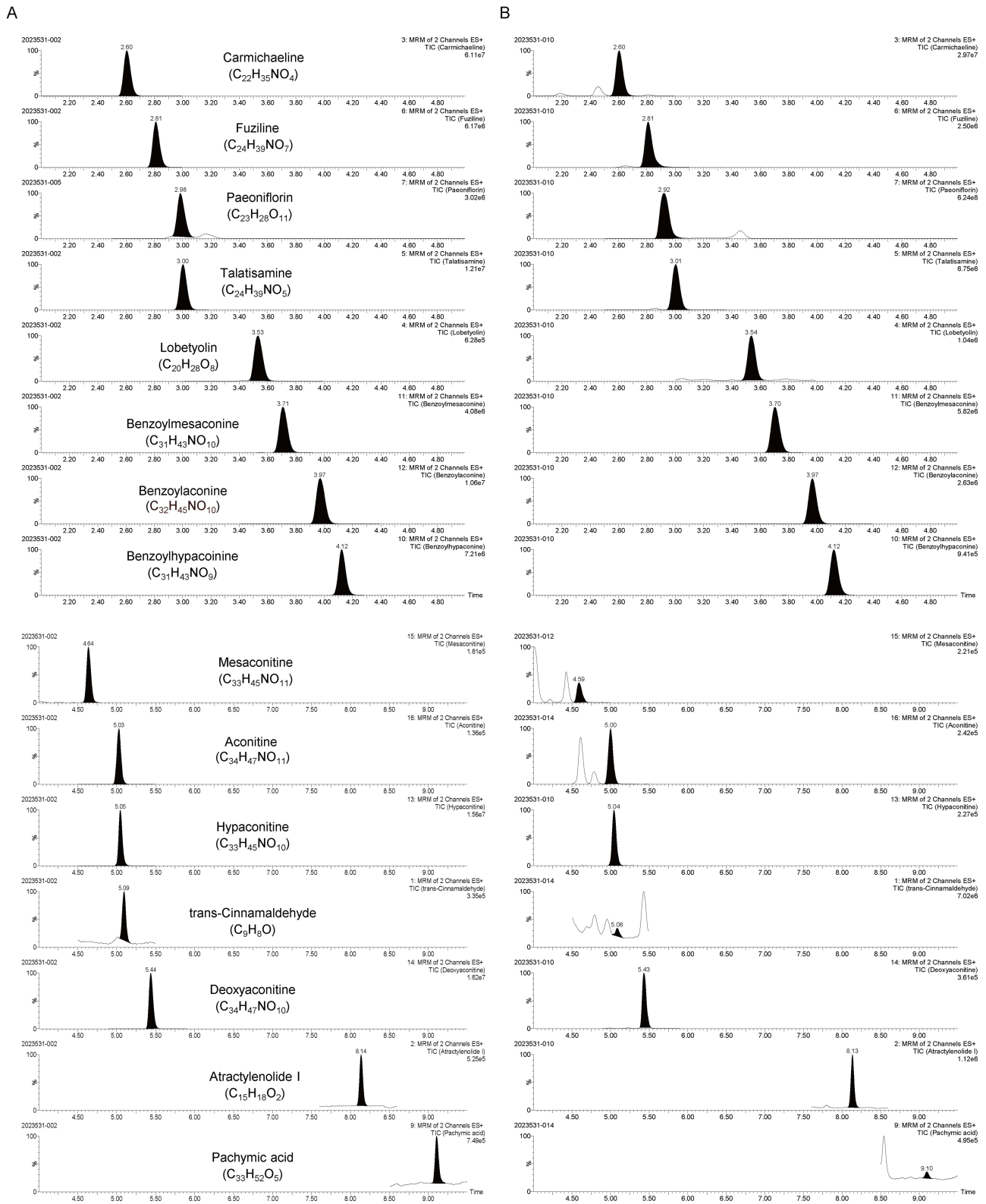

Figure 1 Chemoprofile of MFZD. UPLC-MS/MS analysis of standard chemicals for trans-cinnamaldehyde, atractylenolide I, lobetyolin, paeoniflorin, pachymic acid, carmichaeline, talatisamine, fuziline, benzoylhypacoinine, benzoylmesaconine, benzoylaconine, hypaconitine, deoxyaconitine, mesaconitine, aconitine (**A**) and MFZD extract (**B**).

https://doi.org/10.2147/DDDT.S481770

Anti-OA Efficacy of MFZD

To explore the potential therapeutic effects of MFZD, an OA rat model was established using intra-articular injection of MIA. Histopathological data of cartilage tissues (HE and SO staining in Figure 2A) showed that both chondrocyte content and collagen mass decreased dramatically after modeling and were restored after four weeks of MFZD administration (both low and high doses). MFZD treatment (high dose, MFZD-H) improved the smoothness of the cartilage surface and Mankin score ($p < 0.01$ vs Model) as well (Figure 2B). In addition, PWT was assessed to determine the pain threshold, which could reflect the progression or remission of OA. The data in Figure 2C showed that PWT value of rats in the Model group was lower than that of the Sham group ($p < 0.05$) and was significantly restored by MFZD treatment. These data implied that MFZD generally remedies cartilage destruction and joint pain in experimental OA rats.

Identification of the Targets and Pathways for the Anti-OA Efficacy of MFZD

Based on the chemoprofile of MFZD, shown in Figure 1, network pharmacology analysis was performed to predict the potential anti-OA targets or pathways of MFZD. Thirty-four ingredients (Table 3) of MFZD and 422 corresponding targets were tentatively screened following the predetermined criteria (oral bioavailability is equal to or greater than 30% and drug-likeness is equal to or greater 0.18). At the same time, a total of 2708 OA-related targets were obtained from databases (including OMIM, Drug Bank, Genecards, Disgenet and TTD). The intersection (79 overlapping targets) of

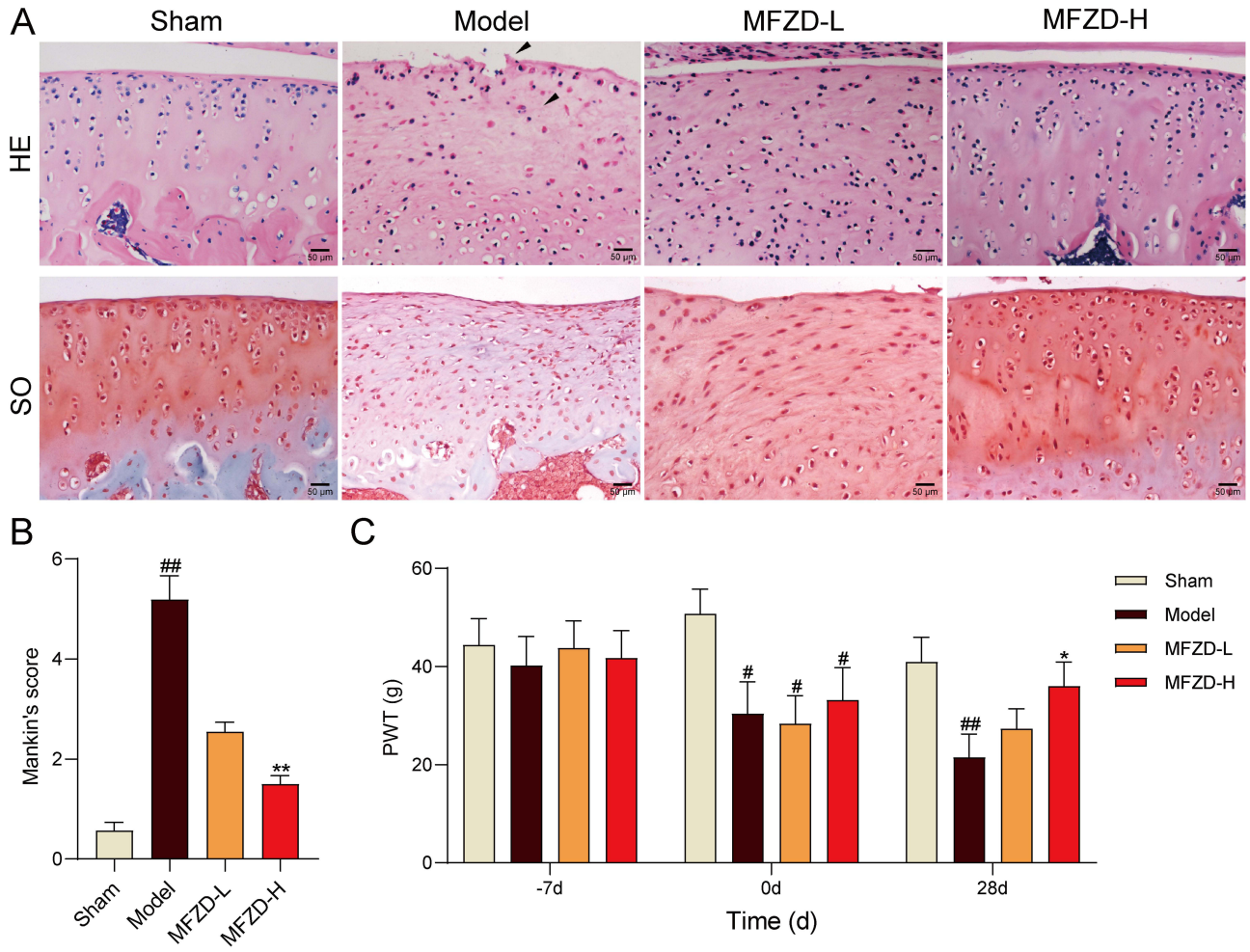

Figure 2 MFZD alleviated the cartilage degeneration of OA in rats. Morphological observation of the cartilage tissues through hematoxylin and eosin (HE) staining (upper), and safranin O/Fast green (SO) staining (lower), scale bars = 50 μm, magnification 40 × (**A**). Mankin's scores for histopathological analysis (**B**) (n = 7) and the paw withdrawal threshold (PWT) determined 7 days before modeling (−7d), on the exact day of modeling (0d), and 28 days after modeling (28d) (**C**) (n = 7). All values were presented as mean ± standard deviation. $^{\#}p < 0.05$ and $^{\#\#}p < 0.01$, vs Sham group; $^{*}p < 0.05$ and $^{**}p < 0.01$, vs Model group. Each repeat was performed as a separate, independent experiment or observation.

Table 3 The Compound Ingredients of MFZD Searched from Indicated Databases

MOLID	Molecule Name	OB (%)	DL	Medicine
MOL001918	Paeoniflorgenone	87.59	0.37	Paeoniae Radix Alba, Paeoniae Radix Rubra
MOL001919	(3S,5R,8R,9R,10S,14S)-3,17-dihydroxy-04,4,8,10,14-pentamethyl -2,3,5,6,7,9-hexahydro-1H-cyclopenta [a] phenanthrene-15,16-dione	43.56	0.53	Paeoniae Radix Alba
MOL001924	Paeoniflorin	53.87	0.79	Paeoniae Radix Alba, Paeoniae Radix Rubra
MOL000358	Beta-sitosterol	36.91	0.75	Paeoniae Radix Alba, Paeoniae Radix Rubra, Cmnamomi Mmulus
MOL000422	Kaempferol	41.88	0.24	Paeoniae Radix Alba
MOL000492	(+)-catechin	54.83	0.24	Paeoniae Radix Alba, Paeoniae Radix Rubra, Cmnamomi Mmulus
MOL000022	14-acetyl-12-senecioyl-2E,8Z,10E-atractylentriol	63.37	0.3	Macrocephalae Rhizoma
MOL000033	(3S,8S,9S,10R,13R,14S,17R)-10,13-dimethyl-17-[(2R,5S)-5-propan-2-yloctan-2-yl]-2,3,4,7,8,9,11,12,14,15,16,17-dodecahydro-1H-cyclopenta [a] phenanthren-3-ol	36.23	0.78	Macrocephalae Rhizoma
MOL000049	3β-acetoxyatractylone	54.07	0.22	Macrocephalae Rhizoma
MOL000072	8β-ethoxy atractylenolide III	35.95	0.21	Macrocephalae Rhizoma
MOL001002	Ellagic acid	43.06	0.43	Paeoniae Radix Rubra
MOL002714	Baicalein	33.52	0.21	Paeoniae Radix Rubra
MOL002776	Baicalin	40.12	0.75	Paeoniae Radix Rubra
MOL000449	Stigmasterol	43.83	0.76	Paeoniae Radix Rubra
MOL006992	(2R,3R)-4-methoxyl-distylin	59.98	0.30	Paeoniae Radix Rubra
MOL003896	7-Methoxy-2-methyl isoflavone	42.56	0.20	Codonopsis Radix
MOL008400	Glycitein	50.48	0.24	Codonopsis Radix
MOL000006	Luteolin	36.16	0.25	Codonopsis Radix
MOL008393	7-(beta-Xylosyl)cephalomannine_qt	38.33	0.29	Codonopsis Radix
MOL007059	3-Beta-Hydroxymethyllenetanshiquinone	32.16	0.41	Codonopsis Radix
MOL006774	Stigmast-7-enol	37.42	0.75	Codonopsis Radix
MOL004355	Spinasterol	42.98	0.76	Codonopsis Radix
MOL008397	Daturilin	50.37	0.77	Codonopsis Radix
MOL000273	16α-Hydroxydehydrotrametenolic acid	30.93	0.81	Poria
MOL000282	Ergosta-7,22E-dien-3beta-ol	43.51	0.72	Poria
MOL000296	Hederagenin	36.91	0.75	Poria
MOL002211	11,14-eicosadienoic acid	39.99	0.2	Aconiti Lateralis Radix Praeparata
MOL002388	Delphin_qt	57.76	0.28	Aconiti Lateralis Radix Praeparata
MOL002392	Deltoin	46.69	0.37	Aconiti Lateralis Radix Praeparata
MOL002395	Deoxyandrographolide	56.30	0.31	Aconiti Lateralis Radix Praeparata
MOL002398	Karanjin	69.56	0.34	Aconiti Lateralis Radix Praeparata
MOL000359	Sitosterol	36.91	0.75	Aconiti Lateralis Radix Praeparata, Cmnamomi Mmulus
MOL001736	(-)-taxifolin	60.51	0.27	Cmnamomi Mmulus
MOL004576	Taxifolin	57.84	0.27	Cmnamomi Mmulus

MFZD and OA was obtained using Venn analysis to identify candidate targets of MFZD in OA intervention (Figure 3A). The compound-target network of MFZD in OA was established using Cytoscape with 223 nodes (7 herbs, 34 ingredients, and 182 targets) and 385 edges (Figure 3G). In the outer circle, active ingredients, including Fuzi, Fuling, Dangshen, Baizhu, Baishao, Chishao, and Guizhi, are displayed in different colors. The PPI network diagram (Figure 3B) shows the anti-OA targets of MFZD, and detailed information of the top 20 core genes is listed in Table 4. The results of GO and

https://doi.org/10.2147/DDDT.S481770

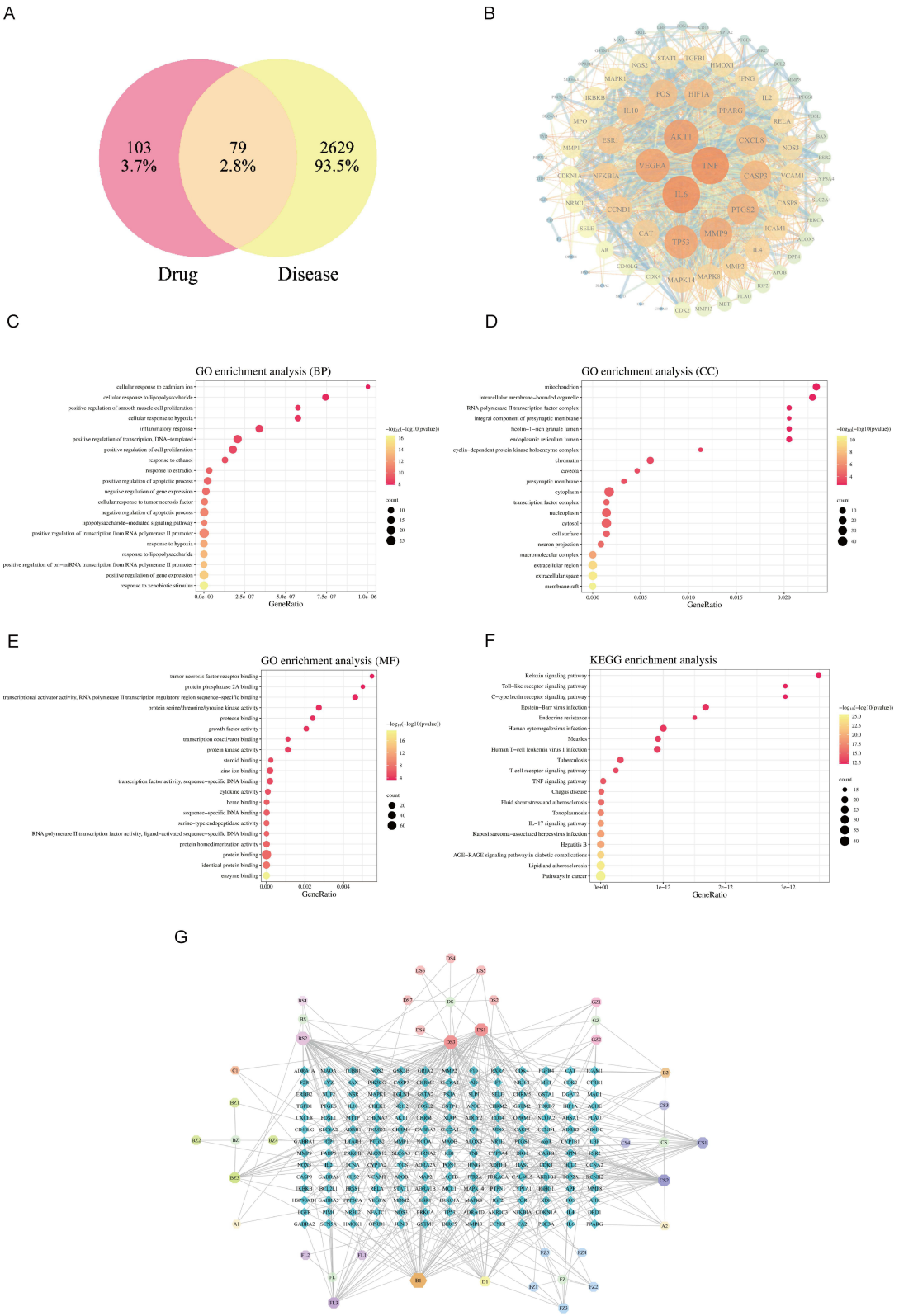

Figure 3 Network pharmacology analysis for potential targets of MFZD in OA therapy. Venn diagram (**A**). The PPI network diagram (**B**). The top 20 significantly enriched terms in biological process (BP) (**C**), cellular component (CC) (**D**) and molecular function (MF) (**E**) through Gene Ontology (GO) analysis. Kyoto Encyclopedia of Genes and Genomes (KEGG) analysis for potential pathways related to the MFZD on OA (**F**). The targets network for seven herbs in MFZD was constructed by linking candidate compounds from the 7 herbs, which were constituents of MFZD, to their putative targets (**G**), the nodes representing candidate compounds were shown as polychromatic hexagons, the targets were indicated by blue rhombus, and the herbs are shown as polychromatic circularity.

Table 4 Top 20 Core Genes of the MFZD-OA PPI Network

Abbreviation	Full Names of the Core Genes	Degree
TNF	Tumor necrosis factor	68
IL-6	Interleukin-6	68
VEGFA	Vascular endothelial growth factor A	62
TP53	Tumor Protein P53	60
MMP9	Matrix metalloproteinase 9	59
PTGS2	Prostaglandin-endoperoxide synthase 2	57
CASP3	Caspase-3	54
CXCL8	C-X-C Motif Chemokine Ligand 8	53
HIF-1	Hypoxia-inducible factor	52
PPARG	Peroxisome proliferator activated receptor gamma	50
FOS	Fos proto-oncogene	49
IL-10	Interleukin-10	47
ESR1	Estrogen receptor 1	46
CAT	Catalase	44
CCND1	Cyclin D 1	44
NFKBIA	NFKB inhibitor alpha	44
MAPK14	Mitogen-activated protein kinase 14	42
MAPK8	Mitogen-activated protein kinase 8	41
IL-4	Interleukin-4	41
MMP2	Matrix metalloproteinase 2	41

KEGG enrichment analyses (Figure 3C–F) indicated that MFZD might exert anti-inflammatory effects in a TNF signaling-related pathway. In addition, potential anti-OA targets of MFZD, such as TNF, IL-6, IKBKB, NFKBIA, STAT1, FOS, and VCAM1, are key molecules involved in TNF-α and/or NF-κB signaling. These data imply that MFZD might play an anti-inflammatory role in OA through TNF-α/NF-κB signaling.

MFZD Prevented the Cartilage Degeneration of OA

Previous studies investigated the protective effects of FZD against OA cartilage degeneration; therefore, MFZD was evaluated for the same efficacy. Immunocytochemical (IHC) analysis of cartilage tissues (Figure 4A and B) showed that MMP13 and Col2 levels in the model group were significantly altered ($p < 0.01$ vs Sham). Compared to the model group, MMP13 and Col2 expression was significantly restored to normal levels in the groups treated with MFZD. To further evaluate the effect of MFZD on cartilage degeneration (hypertrophy and catabolism), total protein was extracted from the cartilage tissues donated by 3 individual rats, and the protein levels of Col10 and MMP13 in the cartilage tissues were evaluated (Figure 4C). As shown, the expression of Col10 and MMP13 was induced in the model group, and MFZD treatment at low and high doses reduced their expression. Despite limited cartilage samples ($n < 5$), the preliminary results in Figure 4C revealed a similar expression pattern of MMP13 with the histological staining data in Figure 4A and B. In sum, these in vivo data indicated that MFZD exerted chondroprotective effects against OA cartilage degeneration.

MFZD Played an Anti-Inflammatory Role Against OA

After modeling, the synovium of the rats showed hyperplastic (villous hyperplasia by HE staining), inflammatory (aggregates of immune-cellular infiltrates by HE staining), and fibrotic (collagen fibrosis by MASSON staining) changes (Figure 5A) with significantly higher Krenn scores (Figure 5B, $p < 0.01$ vs Sham), indicating typical synovial inflammation (synovitis) in OA. MFZD treatment significantly alleviated synovitis induced by the model (Figure 5A and B). To confirm this, serum levels of typical pro-inflammatory cytokines were measured. Serum levels of MCP-1 detected by ELISA (Figure 5C) were significantly induced in the model group ($p < 0.01$ vs Sham) and reduced by treatment with MFZD at both low and high doses ($p < 0.05$ vs Model). Meanwhile, serum levels of TNF-α (Figure 5C) were significantly induced after

https://doi.org/10.2147/DDDT.S481770

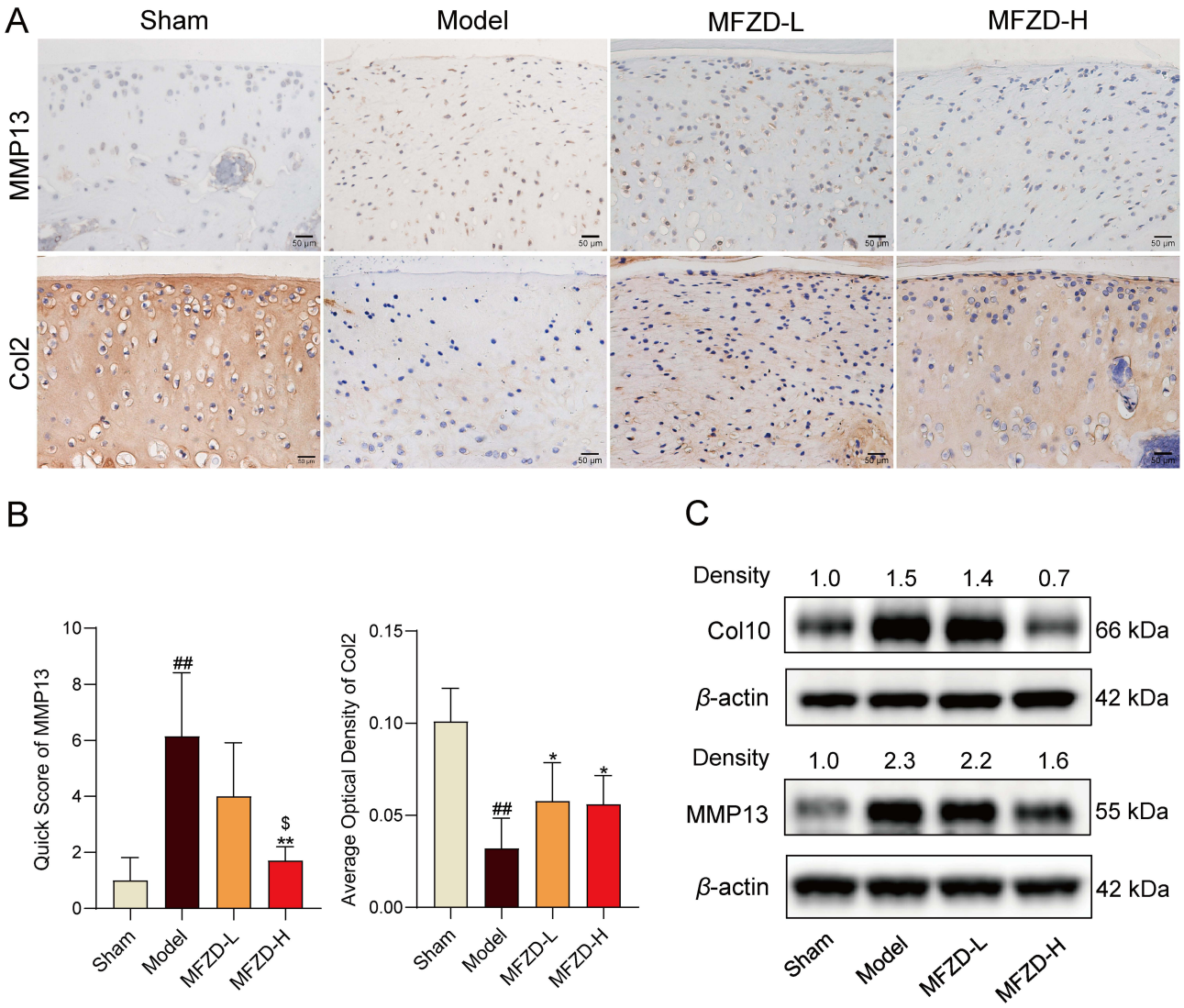

Figure 4 MFZD restored the balance between anabolism and catabolism in rat cartilage tissues. Expressions of MMP13 and Col2 in cartilage evaluated by IHC staining (**A**) and quantitative measurements of positive cells for MMP13 and Col2 (**B**) (n = 7), scale bars = 50 μm, magnification 40 ×. Protein level of Col10 and MMP13 in rat cartilage tissues determined by WB (**C**). All values were presented as mean ± standard deviation. $^{\#\#}p < 0.01$, vs Sham group; $^{*}p < 0.05$ and $^{**}p < 0.01$, vs Model group; $^{\$}p < 0.05$, MFZD-L vs MFZD-H group. Each repeat was performed as a separate, independent experiment or observation.

modeling ($p < 0.01$ vs Sham) and reduced by MFZD treatment at both low dose ($p < 0.05$, vs model) and high dose ($p < 0.01$, vs Model). In addition, TNF-α levels decreased significantly in a dose dependent manner ($p < 0.05$, MFZD-H vs MFZD-L).

MFZD Remedies OA-Related Inflammation via TNF-α/TRAF2/NF-κB Signaling

To further investigate the anti-inflammatory role of MFZD against OA and to verify the mechanism of involvement of the TNF-α-induced TRAF2/NF-κB pathway, immunohistochemistry (IHC) staining of VCAM1 (downstream target of NF-κB, which is responsible for the recruitment of monocytes/macrophages to amplify inflammation) and TRAF2 (adaptor that links TNF-α and NF-κB) in the synovium was performed. Figure 6A and B showed that the expression of VCAM1 and TRAF2 was significantly induced in the synovium, whereas MFZD treatment prevented their expression. In addition, we performed in vitro verification of SFs. In vitro data showed that, the expression of phosphorylated MKK3/MKK6 (p-MKK3/MKK6), phosphorylated p38 (p-p38), TRAF2, phosphorylated p65 (p-p65), and VCAM1 were induced by TNF-α stimulation, which were reversed by MFZD treatment with 5% and/or 10% MFCS (Figure 6C–F). Collectively,

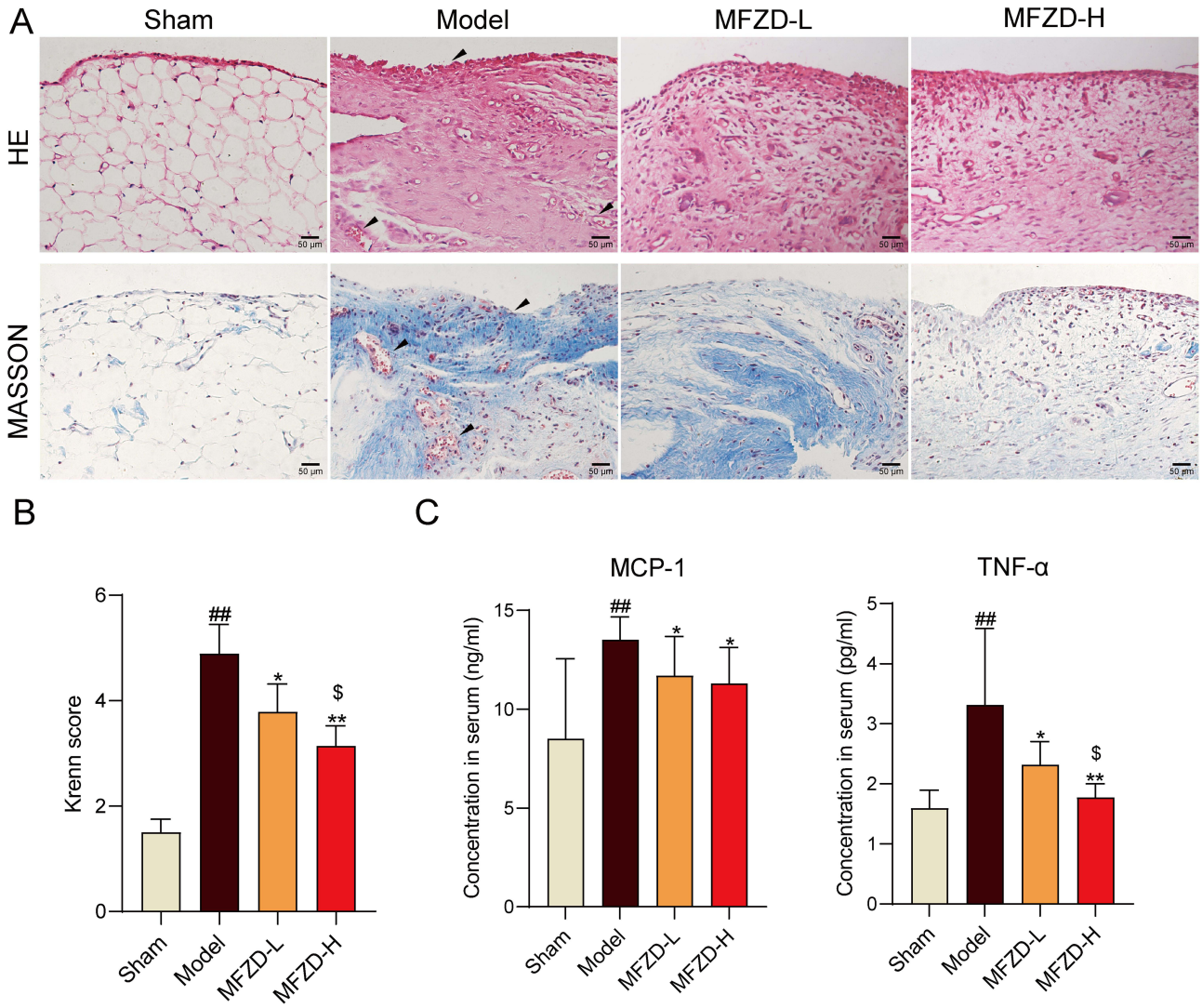

Figure 5 The anti-inflammatory efficacy of MFZD in OA therapy. Histopathological observation of the synovium through hematoxylin and eosin (HE) staining and MASSON staining (**A**) and the relative Krenn scores (**B**) (n = 7), scale bars = 50 μm, magnification 40 ×. Levels of MCP-1 (determined by ELISA) and TNF-α (determined by MSD assay) in the rat serum (**C**) (n = 7). All values were presented as mean ± standard deviation. $^{\#\#}p < 0.01$, vs Sham group; $^{*}p < 0.05$ and $^{**}p < 0.01$, vs Model group; $^{\$}p < 0.05$, MFZD-L vs MFZD-H group. Each repeat was performed as a separate, independent experiment or observation.

these results indicated that MFZD could alleviate the inflammatory status of OA and that the TNF-α/TRAF2/NF-κB signaling pathway is involved in its remedy of synovitis.

Discussion

OA is a chronic degenerative disease characterized by low-grade inflammation. Cartilage degeneration has been reported to be one of the main factors mediating the onset of OA,[46,47] manifested by abnormally activated catabolism, hypertrophic differentiation, and apoptosis in chondrocytes. Previous studies have found that before the appearance of typical imaging lesions, patients with early-stage OA had already suffered from synovitis. Different from the rheumatoid inflammation of RA, OA synovitis is a low-grade chronic inflammation, featured with monocytes infiltration, intimal thickening and secretion of the pro-inflammatory cytokines of the synovium.[48] Synovial fibroblasts under such a chronic inflammatory environment could be further stimulated to produce several adhesion molecules and chemokines (such as VCAM1 and MCP-1) to recruit monocytes/macrophages,[49,50] as well as to release pro-inflammatory cytokines (such as IL-1β, IL-6, TNF-α), matrix enzymes (such as MMPs and ADAMTSs) and neuropeptides.[51,52] Inflammatory cascade reactions above led to chronic synovitis, ECM matrix degradation (ie, cartilage degeneration), pain, etc. to accelerate OA

https://doi.org/10.2147/DDDT.S481770

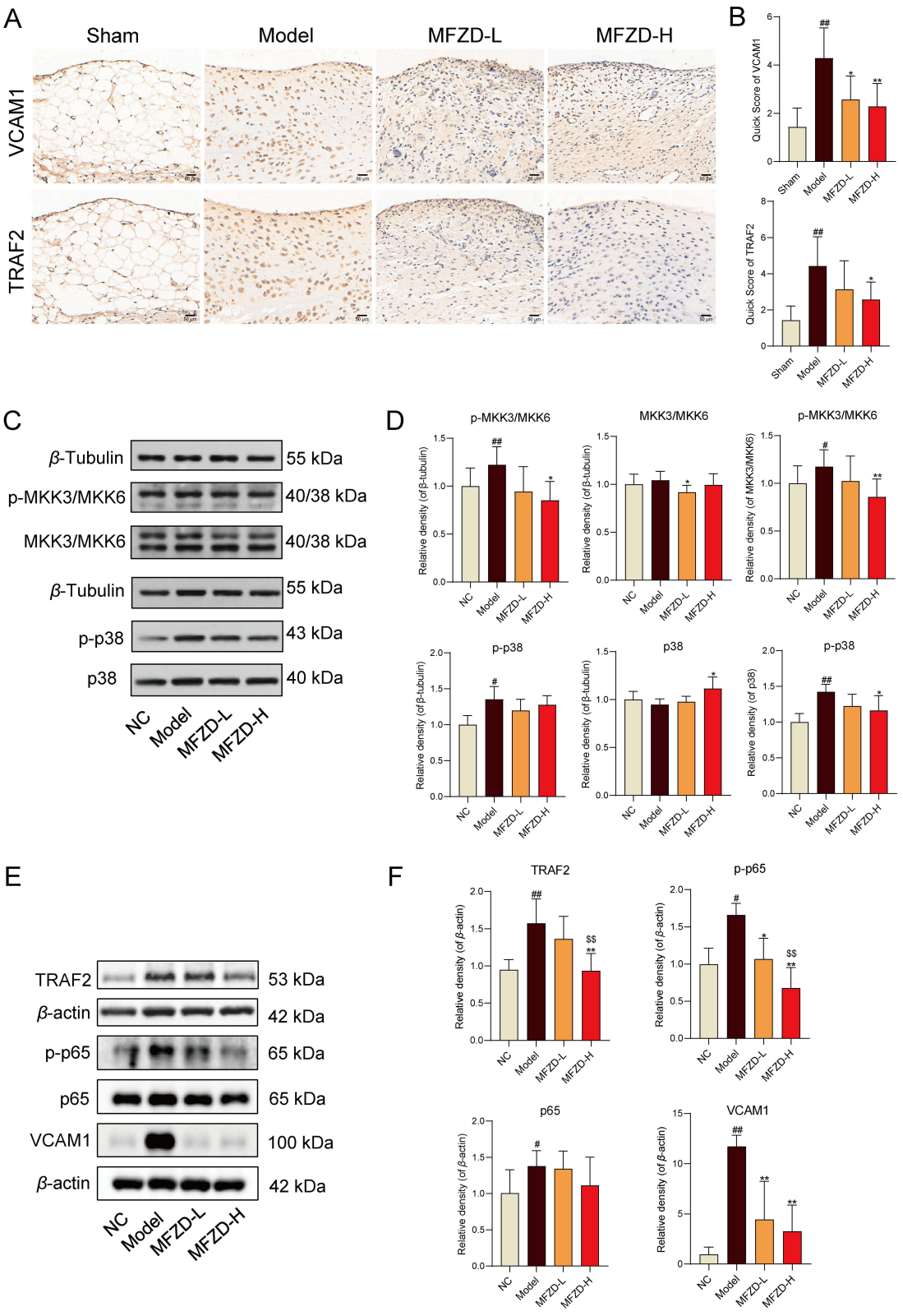

Figure 6 MFZD played an anti-inflammatory role toward OA via inhibiting the synovial TNF-α/TRAF2/NF-κB signaling pathway. Representative immunohistochemical staining of VCAM1 and TRAF2 in the synovium (**A**) and the quantitative measurement of positive cells (**B**) (n = 7), scale bars = 50 μm, magnification 40 ×. Protein levels of p-MKK3/MKK6, MKK3/MKK6, p-p38 and p38 in rat SFs determined by WB (**C**) and the statistical analysis for their relative densities (**D**) (n = 5). Protein levels of TRAF2, p-p65, p65 and VCAM1 in rat SFs determined by WB (**E**) and the statistical analysis for their relative densities (**F**) (n = 5). All values were presented as mean ± standard deviation. $^{\#}p < 0.05$ and $^{\#\#}p < 0.01$, vs Sham group or NC group; $^{*}p < 0.05$, $^{**}p < 0.01$, vs Model group; $^{\$\$}p < 0.01$, MFZD-L vs MFZD-H group. Each repeat was performed as a separate, independent experiment or observation.

progression.[53] Taken together, targeting synovitis might be a potential way to prevent OA progression. Animal models are the primary tools used to study the pathogenesis and intervention mechanisms of OA. Animal models of OA have been established using chemical injections and various surgical procedures. Surgical OA models mainly cause joint wear and are therefore inappropriate for synovitis studies. Thus, to investigate the effects and potential mechanisms of MFZD on OA synovitis and pain, the MIA-induced OA model (a chemical-induced OA model) was selected for this study.[54–56] Nevertheless, due to limited number of animal samples, cartilage tissues from the same side were collected for histological staining, while cartilage tissues from the other side were collected to extract total protein or total ribonucleic acid. Thus, there were only 3 cartilage samples to analyze the protein expression of Col10 and MMP13 (Figure 4C), which is one of the limitations of this study. Preliminary results in Figure 4C hinting that MFZD prevented hypertrophic and catabolic degeneration of the cartilage, were worth to be further investigated.

FZD was first recorded in Treatise on Febrile Diseases (an ancient book named *Treatise on Febrile Diseases* in Chinese) in the Han Dynasty of China. According to the theory of TCM, FZD can be applied to treat arthralgia (including OA) caused by external evils of wind, cold, and dampness. Previous study revealed that FZD could alleviate the symptoms of OA, evidenced by significantly reduced WOMAC and VAS symptom scores in OA patients taking FZD orally in clinic, and prevented cartilage degeneration in OA rat model via inhibiting the PI3K/AKT signaling pathway in chondrocytes.[22] FZD used in the study above contained atractyl enolide I, benzoylhypaconitine, benzoylmesaconitine, benzoylaconitine, hypaconitine, mesaconitine, aconitine, lobetyolin, paeoniflorin, pachymic acid. Several of these, such as benzoylmesaconine, benzoylhypaconine, aconitine, and Fuziline,[33,57] have been reported to have anti-inflammatory properties. Nevertheless, the anti-inflammatory efficacy of the original or modified FZD, which is also beneficial in relieving OA symptoms, remains unclear. The MFZD used in the current study, with additional Guizhi (Cmnamomi Mmulus) and Shaoyao (Paeoniae Radix Rubra), was a supplemented and modified FZD. Bioactive components from Guizhi and Shaoyao, such as cinnamaldehyde and paeoniflorin, were found to have anti-inflammatory properties.[28,58–60] According to the UPLC/MS/MS analysis, MFZD contained additional or even more chemicals or ingredients than FZD, such as trans-cinnamaldehyde, aconite, carmichrin, taradassamine and deoxyaconitine. Thereinto, trans-cinnamaldehyde was detected only in MFZD. Trans-cinnamaldehyde was proved to play certain anti-inflammatory effects on chondrocytes both in vivo and in vitro through NF-κB, p38-JNK and PI3K/AKT pathway;[61] it could also improve foot paw swelling, synovial hyperplasia and inflammatory cell infiltration in rats with adjuvanted arthritis.[62] In addition, cinnamaldehyde exhibits anti-inflammatory properties in OA synovial fibroblasts via the TLR4/Myd88 pathway.[28] In sum, trans-cinnamaldehyde might play a vital role in the anti-inflammatory properties of MFZD against OA, but the underlying mechanisms remain to be elucidated.

The potential anti-inflammatory mechanism of MFZD was explored using a network pharmacology analysis. Targets, such as TNF, IL-6, IKBKB, NFKBIA, STAT1, FOS, and VCAM1, were identified. Related GO enrichment indicated the anti-inflammatory efficacy of MFZD, as evidenced by its impact on the inflammatory response (BP) and tumor necrosis receptor binding (MF). In addition, involvement of the TNF signaling pathway was proposed by KEGG enrichment analysis. TNF-α is a well-known type of TNF secreted by macrophages. It is one of the widely studied pro-inflammatory cytokines involved in the pathophysiology of OA and plays an important role in inflammatory pain and bone lesions.[63] TNF-α activates downstream signaling pathways through adaptors, including TRAF2, to participate in inflammatory responses.[64] NF-κB is one of the downstream pathways of TNF-α, mediating synovitis of arthritis.[65] VCAM1 is one of the downstream target genes of the NF-κB pathway and is responsible for the amplification and acceleration of synovitis by recruiting macrophages during OA progression.[66,67] Collectively, we propose that MFZD ameliorates OA synovitis through multicomponent synergy targeting the TNF-α/TRAF2/NF-κB signaling axis. This synergistic inhibition is substantiated by documented bioactive constituents: Cinnamaldehyde and atractylenolide (including derivatives) suppress TNF-α production via NF-κB inactivation across multiple cellular models;[34–36] Lobetyolin and benzoylaconitine demonstrate NF-κB signaling inhibition;[37,38] Notably, CP-25 (paeoniflorin-6′-O-benzene sulfonate), a patented paeoniflorin derivative, directly attenuates the BAFF-TRAF2-NF-κB cascade, reducing inflammatory indices in collagen-induced arthritis.[68]

In this study, MFZD was found to reduce the serum content of TNF-α and the protein levels of TRAF2 and VCAM1 in the synovium of OA rats, while in vitro study proved that MFZD treatment could prevent TNF-α-induced expression (at the protein level) of TRAF2, p-p65, and VCAM1 in SFs. Thus, we conclude that MFZD plays an anti-inflammatory role against OA by inhibiting the TNF-α/TRAF2/NF-κB signaling pathway in the synovium. MFZD exhibits

considerable potential for clinical application in OA, particularly among patients with magnetic resonance imaging (MRI)-detected synovitis. However, this study is subject to limitations: 1) the specific components within MFZD that modulate the TNF-α/TRAF2/NF-κB signaling have not been elucidated; 2) other pathways beyond the TNF-α/TRAF2/NF-κB signaling were identified but not validated, and their potential contributions to the anti-OA efficacy of MFZD remain unexplored.

Conclusion

This study analyzed the chemoprofile, as well as verified its anti-degenerative and anti-inflammatory efficacy of MFZD against OA. Subsequently, network pharmacology analysis and in vivo and in vitro experiments revealed that MFZD alleviated OA inflammation via inhibition of the TNF-α/TRAF2/NF-κB signaling pathway in the SFs and synovium of rats. The current study confirms that the TCM theory can provide instructive cures for diseases, especially for those without a specific medicine in the clinic. In the future, prospective clinical trials are warranted to evaluate the therapeutic efficacy of MFZD against OA.

Abbreviations

FZD, Fuzi decoction; MFZD, modified Fuzi decoction; OA, osteoarthritis; UPLC-MS/MS, Ultra Performance Liquid Chromatography-Tandem Mass Spectrometry; MIA, mono iodoacetate; ELISA, enzyme-linked immunosorbent assay; MSD, Meso Scale Discovery; WB, Western blot; KEGG, kyoto encyclopedia of genes and genomes; TNF-α, tumor necrosis factor-α; MFCS, MFZD-containing serum; BS, blank serum; PWT, paw withdrawal threshold; MCP-1, monocyte chemotactic protein 1; TCM, traditional Chinese medicine; MRM, multiple reaction monitoring; SPF, specific pathogen free; SD, Sprague Dawley; SFs, synovial fibroblasts; DMEM, Dulbecco's modified eagle medium; HE, hematoxylin and eosin; SO, Safranin O/Fast green; Col2, collagen type II; MMP13, matrix metallopeptidase 13; DAB, diaminobenzidine; Q-score, quick score; AOD, average optical density; TCMSP, Traditional Chinese Medicine Systems Pharmacology Database and Analysis Platform; OMIM, Online Mendelian Inheritance in Man; TTD, therapeutic target database; PPI, protein-protein interaction; GO, gene ontology; CC, cellular component; MF, molecular function; BP, biological process; IHC, immunohistochemistry; BCA, bicinchoninic acid; TBST, tris buffered saline with tween; ANOVA, analysis of variance; p-MKK3/MKK6, phosphorylated MKK3/MKK6; p-p38, phosphorylated p38; p-p65, phosphorylated p65; TRAF2, TNF receptor-associated factor 2; VCAM1, vascular cell adhesion molecule-1.

Ethical Statement

Public databases or platform, including TCMSP, Disgenet, Drugbank, GeneGards, OMIM, and TTD, were used to obtain publicly available data. Due to the involvement of publicly available human data, this study was reviewed by the Institutional Review Board (IRB) of the First Affiliated Hospital of Zhejiang Chinese Medical University (Acceptance number: 2025-KL-399-01) and was approved by the IRB to be exempt from ethical approval basing on item 1 and 2 of Article 32 of the Measures for Ethical Review of Life Science and Medical Research Involving Human Subjects dated February 18, 2023, China.

Acknowledgments

This work was supported by grants from the Natural Science Foundation of China (grant numbers 82104890 and 82274373), Zhejiang Provincial Natural Science Foundation (grant number LY24H270002), Zhejiang Provincial Key Research and Development Program (grant number 2021C03046), Zhejiang Traditional Chinese Medical Science Foundation (grant numbers 2020ZA039 and 2022ZB137), and the Natural Science Foundation of Zhejiang Chinese Medical University (grant numbers 2023JKZKTS29 and 2021JKZDZC05).

We appreciate the great help from the Medical Research Center, Academy of Chinese Medical Sciences, Zhejiang Chinese Medical University. And we also appreciate Shanghai LabEx Biotech Co., LTD., as the whole process of MSD experiment was performed by Shanghai LabEx Biotech Co., LTD. We thank Ms. Siqing Chen from Hangzhou Shangyu Biotechnology Co., Ltd., for her technical support.

Disclosure

The authors report no conflicts of interest in this work.

References

1. Glyn-Jones S, Palmer AJ, Agricola R, et al. Osteoarthritis. *Lancet*. 2015;386(9991):376–387. doi:10.1016/S0140-6736(14)60802-3
2. Yao Q, Wu X, Tao C, et al. Osteoarthritis: pathogenic signaling pathways and therapeutic targets. *Signal Transduct Target Ther*. 2023;8(1):56. doi:10.1038/s41392-023-01330-w
3. Peshkova M, Lychagin A, Lipina M, et al. Gender-related aspects in osteoarthritis development and progression: a review. *Int J Mol Sci*. 2022;23(5):2767. doi:10.3390/ijms23052767
4. Lee YT, Yunus MHM, Ugusman A, Yazid MD. Natural compounds affecting inflammatory pathways of osteoarthritis. *Antioxidants*. 2022;11(9):1722. doi:10.3390/antiox11091722
5. Hunter DJ, Bierma-Zeinstra S. Osteoarthritis. *Lancet*. 2019;393(10182):1745–1759. doi:10.1016/S0140-6736(19)30417-9
6. Nelson AE. Osteoarthritis year in review 2017: clinical. *Osteoarthritis Cartilage*. 2018;26(3):319–325. doi:10.1016/j.joca.2017.11.014
7. Belsey J, Yasen SK, Jobson S, Faulkner J, Wilson AJ. Return to physical activity after high tibial osteotomy or unicompartmental knee arthroplasty: a systematic review and pooling data analysis. *Am J Sports Med*. 2021;49(5):1372–1380. doi:10.1177/0363546520948861
8. Kunze KN, Beletsky A, Hannon CP, et al. Return to work and sport after proximal tibial osteotomy and the effects of opening versus closing wedge techniques on adverse outcomes: a systematic review and meta-analysis. *Am J Sports Med*. 2020;48(9):2295–2304. doi:10.1177/0363546519881638
9. An JS, Mabrouk A, Khakha R, et al. Assessment of return to sport and functional outcomes following distal femoral, double level and high tibial osteotomies for active patients with symptomatic varus malalignment. *Knee Surg Sports Traumatol Arthrosc*. 2023;31(10):4285–4291. doi:10.1007/s00167-023-07457-1
10. Su S, Tian R, Jiao Y, et al. Ubiquitination and deubiquitination: implications for the pathogenesis and treatment of osteoarthritis. *J Orthop Translat*. 2024;49:156–166. doi:10.1016/j.jot.2024.09.011
11. Katz JN, Arant KR, Loeser RF. Diagnosis and treatment of hip and knee osteoarthritis: a review. *JAMA*. 2021;325(6):568–578. doi:10.1001/jama.2020.22171
12. Abramoff B, Caldera FE. Osteoarthritis: pathology, diagnosis, and treatment options. *Med Clin North Am*. 2020;104(2):293–311. doi:10.1016/j.mcna.2019.10.007
13. Liu B, Xian Y, Chen X, et al. Inflammatory fibroblast-like synoviocyte-derived exosomes aggravate osteoarthritis via enhancing macrophage glycolysis. *Adv Sci*. 2024;11(14):e2307338. doi:10.1002/advs.202307338
14. Sellam J, Berenbaum F. The role of synovitis in pathophysiology and clinical symptoms of osteoarthritis. *Nat Rev Rheumatol*. 2010;6(11):625–635. doi:10.1038/nrrheum.2010.159
15. Liang Y, Xu Y, Zhu Y, Ye H, Wang Q, Xu G. Efficacy and safety of chinese herbal medicine for knee osteoarthritis: systematic review and meta-analysis of randomized controlled trials. *Phytomedicine*. 2022;100:154029. doi:10.1016/j.phymed.2022.154029
16. Zhang S, Zhan J, Li M, et al. therapeutic potential of traditional chinese medicine against osteoarthritis: targeting the Wnt signaling pathway. *Am J Chin Med*. 2024;52(7):2021–2052. doi:10.1142/s0192415x24500782
17. Kong X, Ning C, Liang Z, et al. Koumine inhibits IL-1β-induced chondrocyte inflammation and ameliorates extracellular matrix degradation in osteoarthritic cartilage through activation of PINK1/Parkin-mediated mitochondrial autophagy. *Biomed Pharmacother*. 2024;173:116273. doi:10.1016/j.biopha.2024.116273
18. Kuang S, Liu Z, Liu L, et al. Polygonatum sibiricum polysaccharides protect against knee osteoarthritis by inhibiting the TLR2/NF-κB signaling pathway in vivo and in vitro. *Int J Biol Macromol*. 2024;274(Pt 1):133137. doi:10.1016/j.ijbiomac.2024.133137
19. Deng X, Qu Y, Li M, et al. Sakuranetin reduces inflammation and chondrocyte dysfunction in osteoarthritis by inhibiting the PI3K/AKT/NF-κB pathway. *Biomed Pharmacother*. 2024;171:116194. doi:10.1016/j.biopha.2024.116194
20. Jie L, Zhang L, Fu H, et al. Xibining inhibition of the PI3K-AKT pathway reduces M1 macrophage polarization to ameliorate KOA synovial inflammation and nociceptive sensitization. *Phytomedicine*. 2025;136:156281. doi:10.1016/j.phymed.2024.156281
21. Wang KX, Gao Y, Lu C, et al. Uncovering the complexity mechanism of different formulas treatment for rheumatoid arthritis based on a novel network pharmacology model. *Front Pharmacol*. 2020;11:1035. doi:10.3389/fphar.2020.01035
22. Chen Z, Zhou L, Ge Y, et al. Fuzi decoction ameliorates pain and cartilage degeneration of osteoarthritic rats through PI3K-Akt signaling pathway and its clinical retrospective evidence. *Phytomedicine*. 2022;100:154071. doi:10.1016/j.phymed.2022.154071
23. Li F, Guo C, Zhang S, Zheng B, Sun K, Shi J. Exploring the role and mechanism of Fuzi decoction in the treatment of osteoporosis by integrating network pharmacology and experimental verification. *J Orthop Surg Res*. 2023;18(1):508. doi:10.1186/s13018-023-03842-1
24. Chen DT, Shen X, Li YM, et al. To explore the mechanism of "Fuzi-Guizhi" for the treatment of osteoarthritis on the basis of network pharmacology and molecular docking. *Comb Chem High Throughput Screen*. 2023;26(4):743–755. doi:10.2174/1386207325666220512000940
25. Wang Y, Chen T, Yang C, et al. Huangqi Guizhi Wuwu Decoction Improves Arthritis and Pathological Damage of Heart and Lung in TNF-Tg Mice. *Front Pharmacol*. 2022;13:871481. doi:10.3389/fphar.2022.871481
26. Zhang Q, Peng W, Wei S, et al. Guizhi-Shaoyao-Zhimu decoction possesses anti-arthritic effects on type II collagen-induced arthritis in rats via suppression of inflammatory reactions, inhibition of invasion & migration and induction of apoptosis in synovial fibroblasts. *Biomed Pharmacother*. 2019;118:109367. doi:10.1016/j.biopha.2019.109367
27. Gunawardena D, Karunaweera N, Lee S, et al. Anti-inflammatory activity of cinnamon (C. zeylanicum and C. cassia) extracts - identification of E-cinnamaldehyde and o-methoxy cinnamaldehyde as the most potent bioactive compounds. *Food Funct*. 2015;6(3):910–919. doi:10.1039/c4fo00680a
28. Chen P, Zhou J, Ruan A, Zeng L, Liu J, Wang Q. Cinnamic Aldehyde, the main monomer component of Cinnamon, exhibits anti-inflammatory property in OA synovial fibroblasts via TLR4/MyD88 pathway. *J Cell Mol Med*. 2022;26(3):913–924. doi:10.1111/jcmm.17148
29. Wu Y, Ying J, Zhu X, Xu C, Wu L. Pachymic acid suppresses the inflammatory response of chondrocytes and alleviates the progression of osteoarthritis via regulating the Sirtuin 6/NF-kappaB signal axis. *Int Immunopharmacol*. 2023;124(Pt A):110854. doi:10.1016/j.intimp.2023.110854

30. Xie Q, Hu X, Zhao X, et al. Effects and mechanism of extracts rich in phenylpropanoids-polyacetylenes and polysaccharides from Codonopsis Radix on improving scopolamine-induced memory impairment of mice. *J Ethnopharmacol*. 2023;319(Pt 1):117106. doi:10.1016/j.jep.2023.117106
31. Wei C, Wang H, Sun X, et al. Pharmacological profiles and therapeutic applications of pachymic acid (Review). *Exp Ther Med*. 2022;24(3):547. doi:10.3892/etm.2022.11484
32. Zhang L, Wei W. Anti-inflammatory and immunoregulatory effects of paeoniflorin and total glucosides of paeony. *Pharmacol Ther*. 2020;207:107452. doi:10.1016/j.pharmthera.2019.107452
33. He G, Wang X, Liu W, et al. Chemical constituents, pharmacological effects, toxicology, processing and compatibility of Fuzi (lateral root of Aconitum carmichaelii Debx): a review. *J Ethnopharmacol*. 2023;307:116160. doi:10.1016/j.jep.2023.116160
34. Park JM, Park JE, Park JS, et al. Anti-inflammatory and antioxidant mechanisms of coniferaldehyde in lipopolysaccharide-induced neuroinflammation: involvement of AMPK/Nrf2 and TAK1/MAPK/NF-κB signaling pathways. *Eur J Pharmacol*. 2024;979:176850. doi:10.1016/j.ejphar.2024.176850
35. Sankaranarayanan J, Lee SC, Kim HK, Kang JY, Kuppa SS, Seon JK. Cinnamaldehyde-mediated suppression of MMP-13, COX-2, and IL-6 through MAPK and NF-κB signaling inhibition in chondrocytes and synoviocytes under inflammatory conditions. *Int J Mol Sci*. 2024;25(23):12914. doi:10.3390/ijms252312914
36. Dai TT, Fang W, Zhu WT, et al. Atractylenolide III ameliorates DSS-induced colitis by improving intestinal epithelial barrier via suppressing the NF-κB-mediated MLCK-pMLC signaling pathway. *Food Chem Toxicol*. 2025;196:115158. doi:10.1016/j.fct.2024.115158
37. Xiu C, Luo H, Huang W, et al. Lobetyolin suppressed osteoclastogenesis and alleviated bone loss in ovariectomy-induced osteoporosis via hindering p50/p65 nuclear translocation and downstream NFATc1/c-Fos expression. *Drug Des Devel Ther*. 2025;19:4689–4715. doi:10.2147/dddt.S515930
38. Zhang QQ, Chen QS, Feng F, Cao X, Chen XF, Zhang H. Benzoylaconitine: a promising ACE2-targeted agonist for enhancing cardiac function in heart failure. *Free Radic Biol Med*. 2024;214:206–218. doi:10.1016/j.freeradbiomed.2024.02.010
39. He L, He T, Xing J, et al. Bone marrow mesenchymal stem cell-derived exosomes protect cartilage damage and relieve knee osteoarthritis pain in a rat model of osteoarthritis. *Stem Cell Res Ther*. 2020;11(1):276. doi:10.1186/s13287-020-01781-w
40. Ru J, Li P, Wang J, et al. TCMSP: a database of systems pharmacology for drug discovery from herbal medicines. *J Cheminform*. 2014;6:13. doi:10.1186/1758-2946-6-13
41. Bateman A, Martin M-J, Orchard S. UniProt: the Universal Protein Knowledgebase in 2025. *Nucleic Acids Res*. 2025;53(D1):D609–D617. doi:10.1093/nar/gkae1010
42. Knox C, Wilson M, Klinger CM, et al. DrugBank 6.0: the DrugBank Knowledgebase for 2024. *Nucleic Acids Res*. 2024;52(D1):D1265–D1275. doi:10.1093/nar/gkad976
43. Rappaport N, Twik M, Plaschkes I, et al. MalaCards: an amalgamated human disease compendium with diverse clinical and genetic annotation and structured search. *Nucleic Acids Res*. 2017;45(D1):D877–D887. doi:10.1093/nar/gkw1012
44. Piñero J, Bravo À, Queralt-Rosinach N, et al. DisGeNET: a comprehensive platform integrating information on human disease-associated genes and variants. *Nucleic Acids Res*. 2017;45(D1):D833–D839. doi:10.1093/nar/gkw943
45. Zhou Y, Zhang Y, Zhao D, et al. TTD: therapeutic target database describing target druggability information. *Nucleic Acids Res*. 2024;52(D1):D1465–d1477. doi:10.1093/nar/gkad751
46. Liu D, Cai ZJ, Yang YT, et al. Mitochondrial quality control in cartilage damage and osteoarthritis: new insights and potential therapeutic targets. *Osteoarthritis Cartilage*. 2022;30(3):395–405. doi:10.1016/j.joca.2021.10.009
47. Fujii Y, Liu L, Yagasaki L, Inotsume M, Chiba T, Asahara H. Cartilage homeostasis and osteoarthritis. *Int J Mol Sci*. 2022;23(11):6316. doi:10.3390/ijms23116316
48. Mathiessen A, Conaghan PG. Synovitis in osteoarthritis: current understanding with therapeutic implications. *Arthritis Res Ther*. 2017;19(1):18. doi:10.1186/s13075-017-1229-9
49. Chen WC, Lin CY, Kuo SJ, et al. Resistin enhances VCAM-1 expression and monocyte adhesion in human osteoarthritis synovial fibroblasts by inhibiting MiR-381 expression through the PKC, p38, and JNK signaling pathways. *Cells*. 2020;9(6):1369. doi:10.3390/cells9061369
50. Lin W, Shen P, Huang Y, et al. Wutou decoction attenuates the synovial inflammation of collagen-induced arthritis rats via regulating macrophage M1/M2 type polarization. *J Ethnopharmacol*. 2023;301:115802. doi:10.1016/j.jep.2022.115802
51. Zhang H, Cai D, Bai X. Macrophages regulate the progression of osteoarthritis. *Osteoarthritis Cartilage*. 2020;28(5):555–561. doi:10.1016/j.joca.2020.01.007
52. Grässel S, Muschter D. Do neuroendocrine peptides and their receptors qualify as novel therapeutic targets in osteoarthritis? *Int J Mol Sci*. 2018;19(2):367. doi:10.3390/ijms19020367
53. Silawal S, Triebel J, Bertsch T, Schulze-Tanzil G. Osteoarthritis and the Complement Cascade. *Clin Med Insights Arthritis Musculoskelet Disord*. 2018;11:1179544117751430. doi:10.1177/1179544117751430
54. Lampropoulou-Adamidou K, Lelovas P, Karadimas EV, et al. Useful animal models for the research of osteoarthritis. *Eur J Orthop Surg Traumatol*. 2014;24(3):263–271. doi:10.1007/s00590-013-1205-2
55. Micheli L, Ghelardini C, Lucarini E, et al. Intra-articular mucilages: behavioural and histological evaluations for a new model of articular pain. *J Pharm Pharmacol*. 2019;71(6):971–981. doi:10.1111/jphp.13078
56. de Sousa Valente J. The pharmacology of pain associated with the monoiodoacetate model of osteoarthritis. *Front Pharmacol*. 2019;10:974. doi:10.3389/fphar.2019.00974
57. Li X, Hou W, Lin T, et al. Neoline, fuziline, songorine and 10-OH mesaconitine are potential quality markers of Fuzi: in vitro and in vivo explorations as well as pharmacokinetics, efficacy and toxicity evaluations. *J Ethnopharmacol*. 2023;303:115879. doi:10.1016/j.jep.2022.115879
58. Yu MX, Ma XQ, Song X, et al. Validation of the key active ingredients and anti-inflammatory and analgesic effects of Shenjin Huoxue mixture against osteoarthritis by integrating network pharmacology approach and thin-layer chromatography analysis. *Drug Des Devel Ther*. 2020;14:1145–1156. doi:10.2147/DDDT.S243951
59. Tseng SH, Lee CJ, Chen SH, et al. Cinnamic aldehyde, an anti-inflammatory component in Du-Huo-Ji-Sheng-Tang, ameliorates arthritis in II collagenase and monosodium iodoacetate induced osteoarthritis rat models. *J Tradit Complement Med*. 2023;13(1):51–61. doi:10.1016/j.jtcme.2022.10.003

60. Chen P, Ruan A, Zhou J, et al. Cinnamic aldehyde inhibits lipopolysaccharide-induced chondrocyte inflammation and reduces cartilage degeneration by blocking the nuclear factor-Kappa B signaling pathway. *Front Pharmacol*. 2020;11:949. doi:10.3389/fphar.2020.00949
61. Xia T, Gao R, Zhou G, Liu J, Li J, Shen J. Trans-cinnamaldehyde inhibits IL-1β-stimulated inflammation in chondrocytes by suppressing NF-κB and p38-JNK pathways and exerts chondrocyte protective effects in a rat model of osteoarthritis. *Biomed Res Int*. 2019;2019:4039472. doi:10.1155/2019/4039472
62. Wan J, Wang SM, Gui ZP, et al. Phytantriol-based lyotropic liquid crystal as a transdermal delivery system. *Eur J Pharm Sci*. 2018;125:93–101. doi:10.1016/j.ejps.2018.09.018
63. Yu H, Huang T, Lu WW, Tong L, Chen D. Osteoarthritis Pain. *Int J Mol Sci*. 2022;23(9). doi:10.3390/ijms23094642
64. Sun K, Guo Z, Zhang J, et al. Inhibition of TRADD ameliorates chondrocyte necroptosis and osteoarthritis by blocking RIPK1-TAK1 pathway and restoring autophagy. *Cell Death Discov*. 2023;9(1):109. doi:10.1038/s41420-023-01406-0
65. Wang Q, Zhou X, Zhao Y, et al. Polyphyllin I ameliorates collagen-induced arthritis by suppressing the inflammation response in macrophages through the NF-κB pathway. *Front Immunol*. 2018;9:2091. doi:10.3389/fimmu.2018.02091
66. Sayegh S, El Atat O, Diallo K, et al. Rheumatoid synovial fluids regulate the immunomodulatory potential of adipose-derived mesenchymal stem cells through a TNF/NF-κB-dependent mechanism. *Front Immunol*. 2019;10:1482. doi:10.3389/fimmu.2019.01482
67. Kurowska-Stolarska M, Alivernini S. Synovial tissue macrophages in joint homeostasis, rheumatoid arthritis and disease remission. *Nat Rev Rheumatol*. 2022;18(7):384–397. doi:10.1038/s41584-022-00790-8
68. Shu JL, Zhang XZ, Han L, et al. Paeoniflorin-6'-O-benzene sulfonate alleviates collagen-induced arthritis in mice by downregulating BAFF-TRAF2-NF-κB signaling: comparison with biological agents. *Acta Pharmacol Sin*. 2019;40(6):801–813. doi:10.1038/s41401-018-0169-5